GFDM Interference Mitigation Without Noise Enhancement

Mohammad Towliat and Seyyed Mohammad Javad Asgari Tabatabaee

***Abstract*— Generalized frequency division multiplexing (GFDM) is a promising candidate for the next generation of wireless communications. Using non-orthogonal pulse shapes in GFDM, the transmitted symbols overlap on each other according to a self-interference matrix. Because of those small singular values of this matrix, the interference compensation leads to noise enhancements at the receiver of GFDM. In this letter, we develop a novel scheme called coded GFDM (CGFDM) that transmits a coded version of symbols. It is shown that the self-interference matrix of CGFDM is unitary with the singular values all equal to one; as a result, the interference removal does not enhance the power of noise.**

***Index Terms*— GFDM, coded GFDM, interference mitigation, noise enhancement.**

I. Introduction

In THE recent past, the generalized frequency division multiplexing (GFDM) system has been introduced in [1], as an alternative to orthogonal frequency division multiplexing (OFDM). The background idea of GFDM is filtering each subcarrier with a well-localized prototype filter to reduce the out of band emission (OOB) [2]. GFDM can appropriately adapt to multi-input multi-output (MIMO) channels [2]. In addition, this system is designed such that a cyclic prefix (CP) is used per a large number of transmitted symbols, instead of appending a CP per each symbol performed in OFDM. As a result, the GFDM bandwidth efficiency can be dramatically higher than that of OFDM [3]. On the other hand, the non-orthogonal nature of GFDM leads to self-interference among the transmitted symbols, which must be compensated at the receiver. There are three types of receivers available for GFDM: zero forcing (ZF), matched filter (MF) and minimum mean square error (MMSE) receivers [2]. In these receivers, those small singular values of the self-interference matrix lead to the noise enhancement and degrade the performance of the interference removal process.

Addressing these considerations, in this article we develop an innovative GFDM-based system which transmits a coded version of symbols and is titled as coded GFDM (CGFDM). We show that CGFDM provides a unitary self-interference matrix with the singular values all equal to one. In this regard, a less complicated MF receiver can be employed to remove the interference completely, without any noise enhancement. The rest of this letter is organized as follows. In the next section, the GFDM system model is studied. Section III presents the proposed CGFDM scheme. Simulation results are reported in Section IV and finally, Section V concludes this letter.

Notations: $\mathbf{I}_N$ and $\mathbf{0}_N$ are the $N \times N$ identity and zero matrices, respectively. Also, $||.||$ denotes the matrix norm.

Manuscript received December 10, 2017; revised January 27, 2018; accepted February 26, 2018. Date of publication March 8, 2018; date of current version May 8, 2018. The associate editor coordinating the review of this paper and approving it for publication was B. Smida. *(Corresponding author: Seyyed Mohammad Javad Asgari Tabatabaee.)*

M. Towliat is with the Department of Electrical Engineering, Ferdowsi University of Mashhad, Mashhad 9177948974, Iran (e-mail: mohammad.toliat@mail.um.ac.ir).

S. M. J. Asgari Tabatabaee is with the Department of Computer and Electrical Engineering, University of Torbat Heydarieh, Torbat Heydarieh 9516168595, Iran (e-mail: s.m.j.asgaritabatabaee@torbath.ac.ir).

Digital Object Identifier 10.1109/LCOMM.2018.2813393

II. GFDM System Model

Consider a GFDM system which is designed to transmit a symbol block of the length K time instances and width L subchannels (*i.e.* $K \times L$ symbol block). In this regard, the output of the GFDM transmitter synthesis filter-bank is given as [2]

$$s[m] = \sum_{k=0}^{K-1} \sum_{l=0}^{L-1} d_{k,l} g_{k,l}[m], \tag{1}$$

in which $d_{k,l}$ is the transmitted symbol at the kth time instance and lth subchannel. Also $g_{k,l}[m]$ is the circular time-frequency shifted version of the prototype filter $g[m]$ as

$$g_{k,l}[m] \triangleq g[(m-kL)_N]\, e^{j2\pi ml/L}, \tag{2}$$

where $N \triangleq KL$ and $(.)_N$ is the modulo operator. Note that, according to (2), in GFDM the shifting step is L and $1/L$ in time and frequency domains, respectively. In a matrix formulation, all elements of the transmitted symbol block are organized in a single vector as $\vec{d} \triangleq [\vec{d}_0^T, \dots \vec{d}_{K-1}^T]^T$, in which for $k = 0, \dots K-1$, $\vec{d}_k \triangleq [d_{k,0}, \dots d_{k,L-1}]^T$ is a vector containing the symbols of all subchannels at time instance k. Note that $\vec{d}$ and $\vec{d}_k$ are of the size $N \times 1$ and $L \times 1$, respectively. By considering (1), the vectorized $s[m]$ for $m = 0, \dots N-1$, can be written as $\vec{s} = \mathbf{A}\vec{d}$, where $\vec{s} \triangleq [s[0], \dots s[N-1]\ ]^T$ and $\mathbf{A}$, of the size $N \times N$, is the self-interference matrix of GFDM defined as

$$\mathbf{A} \triangleq [\mathbf{G}_0, \mathbf{G}_1, \dots \mathbf{G}_{K-1}], \tag{3}$$

in which $\mathbf{G}_k$, for $k = 0, \dots K-1$, is the $N \times L$ matrix of $g_{k,l}[m]$ coefficients, such that

$$\mathbf{G}_k = \begin{bmatrix} g_{k,0}[0] & \dots & g_{k,L-1}[0] \\ \vdots & \ddots & \vdots \\ g_{k,0}[N-1] & \dots & g_{k,L-1}[N-1] \end{bmatrix}. \tag{4}$$

According to the GFDM procedure, before transmission through the channel, a CP is appended to $\vec{s}$ to avoid the overlap between two consecutive transmitted symbol blocks. At the receiver, after removing the CP, the resulted vector becomes [3]

$$\vec{y} = \mathbf{H}\vec{s} + \vec{w} = \mathbf{H}\mathbf{A}\vec{d} + \vec{w}, \tag{5}$$

where $\vec{w}$ is the additive noise vector and $\mathbf{H}$ is the $N \times N$ circular matrix of the channel coefficients. In order to estimate the transmitted symbols, the receiver matrix $\mathbf{Q}$ is multiplied by $\vec{y}$, such that the estimated version of the transmitted symbol vector $\vec{d}$ is obtained as $\hat{\vec{d}} = \mathbf{Q}\vec{y}$. There are three types of receivers available for GFDM [2]: *i) ZF receiver*: in which $\mathbf{Q} = (\mathbf{HA})^{-1}$; herein the interference is completely removed but those small singular values of $\mathbf{A}$ increase the power of the resulted noise with the noise enhancement factor (NEF) $\eta_{\mathrm{GFDM}} \triangleq \|\mathbf{A}^{-1}\|^2$ [4]. Note that, since $\mathbf{A}$ is a normalized matrix (*i.e.* $||\mathbf{A}||^2 = 1$), the ideal quantity for NEF (which ends to no enhancement on the noise) is $\eta_{\mathrm{GFDM}} = 1$. In GFDM, this ideal NEF is achievable only if the prototype pulse has a perfect *rectangular* or *sinc* shape. Since in these cases none of the motivations of GFDM is fulfilled, it can be said that it is practically impossible to achieve the ideal NEF in GFDM and we have always $\eta_{\mathrm{GFDM}} > 1$ [4]. *ii) MF receiver*: in which $\mathbf{Q} = \mathbf{A}^H\mathbf{H}^{-1}$. The MF receiver does not enhance the noise (since $||\mathbf{A}^H||^2 = 1$) but because of non-orthogonality of $\mathbf{A}$ (*i.e.* $\mathbf{A}^H\mathbf{A} \neq \mathbf{I}_N$), it cannot completely remove the interference. In this regard, an extra successive interference canceller (SIC) is needed to work along with the MF receiver to mitigate the residual interference after the matched filtering. The combination of MF and SIC is known as the MFSIC receiver [5]. *iii) MMSE receiver*: where $\mathbf{Q} = (\mathbf{R}_w + \mathbf{A}^H\mathbf{H}^H\mathbf{HA})^{-1}\mathbf{A}^H\mathbf{H}^H$ and $\mathbf{R}_w$ is the noise covariance matrix. The MMSE receiver makes a compromise between interference removal and noise enhancement and leads to a better performance compared to the ZF and simple MF receivers [2]. As we discussed, none of the available receivers for GFDM are capable to mitigate the interference completely, without any noise enhancement. Addressing this concern, in the following section we develop our novel CGFDM system, in which the self-interference matrix becomes unitary and it is guaranteed that the interference can be completely mitigated, while there is no noise enhancement.

III. The Proposed CGFDM System

The symbols in CGFDM are organized to be transmitted via two consecutive symbol blocks, both of them with the length $2K$ time instances and width L subchannels (two $2K \times L$ symbol blocks). According to the proposed CGFDM, the transmission of these two symbol blocks is performed as below:

A. Transmission of the First Symbol Block

The transmitter synthesis filter-bank output for the first symbol block is constructed as

$$s'[m] = \sum_{k=0}^{2K-1}\sum_{l=0}^{L-1} d'_{k,l}\, g'_{k,l}[m], \tag{6}$$

where $d'_{k,l}$ is the transmitted symbol at the kth time instance and lth subchannel. Also, $g'_{k,l}[m]$ is the circular time-frequency shifted version of $g[m]$ such that

$$g'_{k,l}[m] \triangleq \frac{1}{\sqrt{2}}\, g[(m - kL/2)_N]e^{j2\pi ml/L}. \tag{7}$$

Note that in (7) the utilized prototype filter is the same as that used in (2), but one difference between $g_{k,l}[m]$ and $g'_{k,l}[m]$ is that in the first one, the time-domain shifting step is L; in contrast, in the latter this step is $L/2$. Also, note that the shifting steps in $g'_{k,l}[m]$ are similar to that of the filter-bank multicarrier/offset QAM (FBMC/OQAM) scheme, in which real-valued symbols are transmitted [6]. Instead, in our derivations in (6), the transmitted symbols $d'_{k,l}$ are complex-valued and accordingly, in (7) the factor $1/\sqrt{2}$ is considered to normalized the power of $s'[m]$, exactly equivalent to that of $s[m]$. Nevertheless, in a matrix presentation, let's define the symbol vector as $\vec{d}' \triangleq [\vec{d}_0'^T, \ldots \vec{d}'^T_{2K-1}]^T$, in which for $k = 0, \ldots 2K-1$, $\vec{d}'_k \triangleq [\vec{d}'_{k,0}, \ldots \vec{d}'_{k,L-1}]^T$. Note that $\vec{d}'$ and $\vec{d}'_k$ are of the size $2N \times 1$ and $L \times 1$, respectively. As a result, according to (6), the transmitted vector $\vec{s}' \triangleq [\, s'[0], \ldots s'[N-1]\,]^T$, of the size $N \times 1$, becomes $\vec{s}' = \mathbf{A}'\vec{d}'$, where $\mathbf{A}'$, of the size $N \times 2N$, presents the CGFDM self-interference matrix of the first symbol block, and is defined as

$$\mathbf{A}' \triangleq [\mathbf{G}'_0, \mathbf{G}'_1, \ldots \mathbf{G}'_{2K-1}]. \tag{8}$$

In (8), for $k = 0, \ldots 2K-1$, $\mathbf{G}'_k$ is the $N \times L$ matrix constructed from coefficients of $g'_{k,l}[m]$, such that

$$\mathbf{G}'_k = \begin{bmatrix} g'_{k,0}[0] & \cdots & g'_{k,L-1}[0] \\ \vdots & \ddots & \vdots \\ g'_{k,0}[N-1] & \cdots & g'_{k,L-1}[N-1] \end{bmatrix}. \tag{9}$$

In a similar way of Section II, in CGFDM a CP is appended to $\vec{s}'$. After removing the CP at the receiver, the resulted vector yields to

$$\vec{y}' = \mathbf{H}\vec{s}' + \vec{w}' = \mathbf{HA}'\vec{d}' + \vec{w}', \tag{10}$$

where $\vec{w}'$ is the additive noise vector and $\mathbf{H}$ is the channel matrix, similar to that of (5). On the other hand, considering (8), one can rewrite (10) separately for even and odd time slots as

$$\begin{aligned}\vec{y}' = \mathbf{H}\Big([\mathbf{G}'_0, \mathbf{G}'_2, \ldots \mathbf{G}'_{2K-2}]\,[\vec{d}'^T_0, \vec{d}'^T_2, \ldots \vec{d}'^T_{2K-2}]^T \\ + [\mathbf{G}'_1, \mathbf{G}'_3, \ldots \mathbf{G}'_{2K-1}]\,[\vec{d}'^T_1, \vec{d}'^T_3, \ldots \vec{d}'^T_{2K-1}]^T\Big) + \vec{w}'.\end{aligned} \tag{11}$$

Comparing (7) and (2), it is concluded that for even time slots we have $[\mathbf{G}'_0, \mathbf{G}'_2, \ldots \mathbf{G}'_{2K-2}] = \frac{1}{\sqrt{2}}\mathbf{A}$, where $\mathbf{A}$ is the self-interference matrix of GFDM defined in (3). As a result, we can represent (11) as

$$\vec{y}' = \frac{1}{\sqrt{2}}\mathbf{H}(\mathbf{A}\vec{x}'_{ev} + \mathbf{B}\vec{x}'_{od}) + \vec{w}', \tag{12}$$

in which $\mathbf{B} \triangleq \sqrt{2}[\mathbf{G}'_1, \mathbf{G}'_3, \ldots \mathbf{G}'_{2K-1}]$. Also, $\vec{x}'_{ev} \triangleq [\vec{d}_0'^T, \vec{d}_2'^T, \ldots \vec{d}'^T_{2K-2}]^T$ and $\vec{x}'_{od} \triangleq [\vec{d}_1'^T, \vec{d}_3'^T, \ldots \vec{d}'^T_{2K-1}]^T$, both of the size $N \times 1$, are the symbol vectors transmitted at even and odd time slots, respectively.

B. Transmission of the Second Symbol Block

At the second symbol block, instead of $\vec{x}'_{ev}$ and $\vec{x}'_{od}$, the symbol vectors $\vec{x}''_{ev} \triangleq -\mathbf{J}\vec{x}'^*_{od}$ and $\vec{x}''_{od} \triangleq \mathbf{J}\vec{x}'^*_{ev}$ are transmitted at even and odd time slots, respectively. The transmission procedure is performed similar to that of the first block; as a result, instead of (12), the received vector becomes

$$\begin{aligned}\vec{y}'' &= \frac{1}{\sqrt{2}}\mathbf{H}(\mathbf{A}\vec{x}''_{ev} + \mathbf{B}\vec{x}''_{od}) + \vec{w}'' \\ &= \frac{1}{\sqrt{2}}\mathbf{H}(-\mathbf{AJ}\vec{x}'^*_{od} + \mathbf{BJ}\vec{x}'^*_{ev}) + \vec{w}''.\end{aligned} \tag{13}$$

where $\vec{w}''$ is the additive noise vector and $\mathbf{J}$ is an $N \times N$ unitary matrix defined as

$$\mathbf{J} \triangleq \begin{bmatrix} 0 & & 1 \\ & \iddots & \\ 1 & & 0 \end{bmatrix}. \tag{14}$$

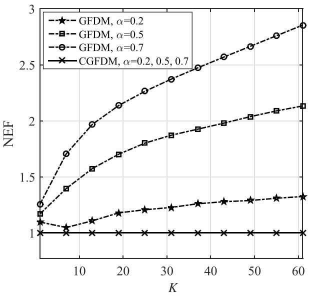

Fig. 1. NEF of GFDM and CGFDM for different values of K and roll-off-factor α.

Concatenating (12) and (13) together, it is concluded that

$$\begin{bmatrix} \vec{y}' \\ \vec{y}''^{*} \end{bmatrix} = \frac{1}{\sqrt{2}} \begin{bmatrix} \mathbf{H} & \mathbf{0}_N \\ \mathbf{0}_N & \mathbf{H}^* \end{bmatrix} \begin{bmatrix} \mathbf{A} & \mathbf{B} \\ \mathbf{B}^*\mathbf{J} & -\mathbf{A}^*\mathbf{J} \end{bmatrix} \begin{bmatrix} \vec{x}'_{ev} \\ \vec{x}'_{od} \end{bmatrix} + \begin{bmatrix} \vec{w}' \\ \vec{w}''^{*} \end{bmatrix}. \tag{15}$$

Let's for more facility, represent (15) as $\vec{Y} = \mathbf{\Xi}\mathbf{\Lambda}\vec{X} + \vec{W}$, in which $\vec{Y} \triangleq [\vec{y}'^{T}, \vec{y}''^{H}]^T$, $\vec{X} \triangleq [\vec{x}'^{T}_{ev}, \vec{x}'^{T}_{od}]^T$, $\vec{W} \triangleq [\vec{w}'^{T}, \vec{w}''^{H}]^T$ and

$$\mathbf{\Xi} \triangleq \begin{bmatrix} \mathbf{H} & \mathbf{0}_N \\ \mathbf{0}_N & \mathbf{H}^* \end{bmatrix}, \quad \mathbf{\Lambda} \triangleq \frac{1}{\sqrt{2}} \begin{bmatrix} \mathbf{A} & \mathbf{B} \\ \mathbf{B}^*\mathbf{J} & -\mathbf{A}^*\mathbf{J} \end{bmatrix}. \tag{16}$$

According to (15), it can be interpreted that $\mathbf{\Lambda}$, of the size $2N \times 2N$, is the total self-interference matrix of CGFDM. We have shown in Appendix that $\mathbf{\Lambda}$ is a unitary matrix, such that $\mathbf{\Lambda}^H\mathbf{\Lambda} = \mathbf{I}_{2N}$; as a result, we can use the simple MF receiver to mitigate the interference completely, such that $\hat{\vec{X}} = \mathbf{Q}\vec{Y}$, where $\hat{\vec{X}}$ is the estimated version of $\vec{X}$ and $\mathbf{Q} \triangleq \mathbf{\Lambda}^H\mathbf{\Xi}^{-1}$ is the MF receiver for CGFDM (MF-CGFDM). On the other hand, since $\mathbf{\Lambda}$ is unitary, the NEF of CGFDM becomes equal to $\eta_{\text{CGFDM}} = \left\|\mathbf{\Lambda}^H\right\| = 1$, which means that the complete interference removal in CGFDM does not inherit any noise enhancement.

Another remarkable point is that in a situation where the length of CP is ϑ, CGFDM transmits two $2K \times L$ symbol blocks, totally during $2N + 2\vartheta$ time slots (see (10), where transmission of each symbol block takes $N + \vartheta$ time slots). But, since the second block is constructed from the symbols of the first block, the CGFDM bandwidth efficiency is $\beta_{\text{CGFDM}} = 2KL/(2N + 2\vartheta)$. In contrast, in the case of GFDM we have $\beta_{\text{GFDM}} = KL/(N+\vartheta)$ (see (5)). As a result, one can conclude that the bandwidth efficiency of CGFDM is exactly equivalent to that of GFDM.

IV. Simulation Results

In this section we compare the performance of CGFDM with that of GFDM and OFDM. But first of all, note that, as it is shown in [4], in GFDM for an even K, the self-interference matrix $\mathbf{A}$ becomes singular. Thus the ZF and MMSE receivers of GFDM cannot be employed when K is even. In this regard, Yoshizawa *et al.* [7] and Nimr *et al.* [8] provide special offset sampling methods for GFDM, to avoid the singularity of $\mathbf{A}$ when K is even. In contrast, in CGFDM, since the self-interference matrix is always unitary, there is no restriction on K and it can set to either even or odd quantities. However, in our simulations, in order to fairly compare CGFDM and GFDM, we consider that K is only odd.

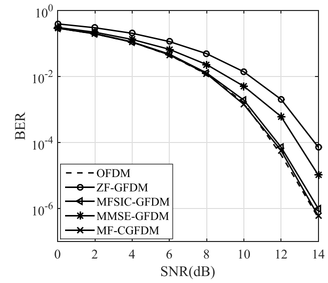

Fig. 2. BER of OFDM, GFDM receivers and MF-CGFDM in AWGN channel.

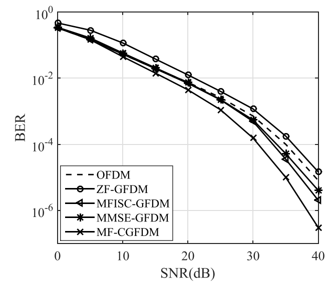

Fig. 3. BER of OFDM, GFDM receivers and MF-CGFDM in frequency selective channel.

Fig. 1 compares the NEF of CGFDM and GFDM, when the prototype pulse shape is root raised cosine (RRC) with the roll-off-factor $\alpha = 0.2$, 0.5 and 0.7, respectively. In this simulation it is considered that $L = 64$ and the NEF is calculated for different values of K. As it can be seen, in GFDM by increasing either α or K the more NEF is resulted; in contrary, in CGFDM the NEF always remains exactly equal to $\eta_{\text{CGFDM}} = 1$, which confirms the unitary property of the CGFDM self-interference matrix. In the following, we compare the bit error rate (BER) performance of MF-CGFDM with that of ZF-GFDM, MFSIC-GFDM (proposed in [5]), MMSE-GFDM and OFDM, versus the signal to noise ratio (SNR). The simulation parameters are considered as follows: modulation is 4-QAM, sampling time $t_s = 100ns$, carrier frequency $f_c = 2GHz$, $L = 64$, $K = 31$ and $\alpha = 0.5$. Also, to ensure that the successive MFSIC-GFDM works well, we set the number of its iterations to $I = 8$ [5]. In our simulations we evaluate the performances when the channel is: *i)* additive white Gaussian noise (AWGN) and, *ii)* frequency selective.

i) Fig. 2 shows the BERs in the AWGN channel. According to these results, the BER performance of MF-CGFDM receiver matches those of OFDM and MFSIC-GFDM, but it is considerably better than the performances of ZF-GFDM and MMSE-GFDM. Obviously, the reason is that, since in CGFDM the self-interference matrix is unitary, the MF-CGFDM completely removes the interference associating no noise enhancement. On the other side, MFSIC-GFDM, with several successive iterations, can approximately approach the performance of MF-CGFDM. In contrast, the noise enhancement in ZF-GFDM and MMSE-GFDM leads to a higher BER.
ii) Fig. 3 compares the BER of the schemes, when the channel is Vehicular-A in the velocity of $V = 100km/h$. Obviously, in such a channel, the performance of MF-CGFDM surpasses those of all GFDM receivers and OFDM. Note that, as it is shown in [2], GFDM-based schemes (*i.e.* GFDM and CGFDM) are potential to outperform OFDM in a frequency

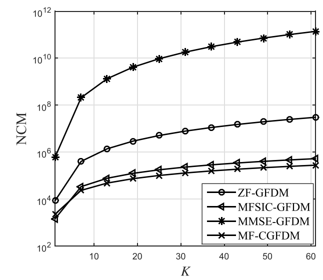

Fig. 4. Comparing the complexities.

selective channel because of their more accurate channel spectrum resolution. The other point is that the MFSIC-GFDM receiver, even with several successive iteration, cannot achieve the performance of the proposed MF-CGFDM.

Evaluating the complexity, Farhang *et al.* [9] present the number of complex multiplications (NCM) for the receivers of GFDM. Furthermore, according to derivations in [9], one can obtain that the NCM of the proposed MF-CGFDM receiver is $2KL(2\log_2 2KL + \log_2 2K + P + 1)$, where P indicates the span of the filter. In this regard, Fig. 4 compares the NCM of all receivers, for different values of K, when $P = 2$ [9]. As it can be seen, although the size of receiver matrix $\mathbf{Q}$ in MF-CGFDM is twice larger than that of GFDM receivers, the NCM of MF-CGFDM is lower. This result is because of the fact that in MF-CGFDM we use a simple matched filter, which does not need any successive iterations.

V. Conclusions

In this article we proposed a novel GFDM-based system called CGFDM which transmits coded symbols with the same bandwidth efficiency as GFDM. The proposed CGFDM provides a unitary self-interference matrix and consequently, a low complicated MF receiver can be used to mitigate the interference completely, without any noise enhancement. Addressing these benefits of CGFDM, the performance of the MF-CGFDM receiver is higher than those of all GFDM receivers, especially in frequency selective channels.

Appendix

In this appendix we will show that $\mathbf{\Lambda}$ is a unitary matrix. In this regard, from (16), we can write

$$\mathbf{\Lambda}^H\mathbf{\Lambda} \triangleq \frac{1}{2}\begin{bmatrix} \mathbf{\Psi} + \mathbf{J}\mathbf{\Phi}^*\mathbf{J} & \mathbf{\Theta} - \mathbf{J}\mathbf{\Theta}^T\mathbf{J} \\ \mathbf{\Theta}^H - \mathbf{J}\mathbf{\Theta}^*\mathbf{J} & \mathbf{\Phi} + \mathbf{J}\mathbf{\Psi}^*\mathbf{J} \end{bmatrix}, \tag{17}$$

where $\mathbf{\Psi} \triangleq \mathbf{A}^H\mathbf{A}$, $\mathbf{\Phi} \triangleq \mathbf{B}^H\mathbf{B}$ and $\mathbf{\Theta} \triangleq \mathbf{A}^H\mathbf{B}$, all of the size $N \times N$. Supposing that the matrix $\mathbf{\Psi}$ is constructed with $L \times L$ sub-matrices $\mathbf{\Psi}^{(k_1,k_2)}$ (for $k_1, k_2 = 0, \ldots K-1$), according to (3), we can conclude that $\mathbf{\Psi}^{(k_1,k_2)} = \mathbf{G}_{k_1}^H\mathbf{G}_{k_2}$. Also from (4), it can be obtained that the (l_1, l_2)th (for $l_1, l_2 = 0, \ldots L-1$) entry of $\mathbf{\Psi}^{(k_1,k_2)}$, which is denoted by $\psi_{l_1,l_2}^{k_1,k_2}$, becomes

$$\begin{aligned}\psi_{l_1,l_2}^{k_1,k_2} &= \sum_{m=0}^{N-1} g_{k_1,l_1}^*[m]\, g_{k_2,l_2}[m] \\ &= \sum_{m=0}^{N-1} g\,[m]\;\; g\left[(m + \Delta k\, L)_N\right] e^{-j2\pi m\, \Delta l/L}. \end{aligned} \tag{18}$$

where $\Delta k \triangleq k_1 - k_2$ and $\Delta l \triangleq l_1 - l_2$. As it can be seen, $\psi_{l_1,l_2}^{k_1,k_2}$ just depends on Δk and Δl; thus, for more facility, we consider that $\psi_{\Delta l}^{\Delta k} \triangleq \psi_{l_1,l_2}^{k_1,k_2}$. In a similar way, $\varphi_{\Delta l}^{\Delta k}$ and $\theta_{\Delta l}^{\Delta k}$ (the (l_1, l_2)th entry of (k_1, k_2)th sub-matrix in $\mathbf{\Phi}$ and $\mathbf{\Theta}$, respectively) can be calculated as

$$\begin{aligned}\varphi_{\Delta l}^{\Delta k} &= (-1)^{\Delta l}\, \psi_{\Delta l}^{\Delta k}, \\ \theta_{\Delta l}^{\Delta k} &\triangleq \sum_{m=0}^{N-1} g\,[m]\, g\left[(m + \Delta k\, L + L/2)_N\right] e^{-j2\pi m\, \Delta l/L}. \end{aligned} \tag{19}$$

Since the entries of $\mathbf{\Psi}$, $\mathbf{\Phi}$ and $\mathbf{\Theta}$ just depend on Δk and Δl, according to the definition of $\mathbf{J}$ in (14), one can derive that $\mathbf{J\Psi J} = \mathbf{\Psi}^T$, $\mathbf{J\Phi J} = \mathbf{\Phi}^T$ and $\mathbf{J\Theta J} = \mathbf{\Theta}^T$. Note that the (l_1, l_2)th entry of (k_1, k_2)th sub-matrix in $\mathbf{\Psi}^T$ is $\psi_{-\Delta l}^{-\Delta k} = \sum_{m=0}^{N-1} g[m]\, g[(m - \Delta k\, L)_N]\, e^{j2\pi m\, \Delta l/L}$; in other words, $\psi_{-\Delta l}^{-\Delta k} = \sum_{m=0}^{N-1} g[(m + \Delta k\, L)_N]\, g[m]\, e^{j2\pi m\, \Delta l/L} = \left(\psi_{\Delta l}^{\Delta k}\right)^*$. As a result, it is concluded that $\mathbf{J\Psi J} = \mathbf{\Psi}^*$. In a similar way, we have $\mathbf{J\Phi J} = \mathbf{\Phi}^*$. In contrast, the (l_1, l_2)th entry of (k_1, k_2)th sub-matrix in $\mathbf{\Theta}^T$ is $\theta_{-\Delta l}^{-\Delta k} = \sum_{m=0}^{N-1} g[m]\, g[(m - \Delta k\, L + L/2)_N]\, e^{j2\pi m\, \Delta l/L} \neq \left(\theta_{\Delta l}^{\Delta k}\right)^*$. As a conclusion, it can be summarized that

$$\mathbf{J\Psi J} = \mathbf{\Psi}^T = \mathbf{\Psi}^*, \quad \mathbf{J\Phi J} = \mathbf{\Phi}^T = \mathbf{\Phi}^*, \quad \mathbf{J\Theta J} = \mathbf{\Theta}^T. \tag{20}$$

By considering (20) into (17), it yields to

$$\mathbf{\Lambda}^H\mathbf{\Lambda} = \frac{1}{2}\begin{bmatrix} \mathbf{\Psi} + \mathbf{\Phi} & \mathbf{0}_N \\ \mathbf{0}_N & \mathbf{\Phi} + \mathbf{\Psi} \end{bmatrix}. \tag{21}$$

On the other hand, since the prototype filter is normalized, we have $\psi_0^0 = 1$. Also when $\Delta l \neq 0$ is even, for each Δk we have a zeros crossing in ambiguity function of the prototype filter (*i.e.* $\psi_{\Delta l}^{\Delta k} = 0$) [10]. As a result, by considering the first term of (19), it is obtained that

$$\psi_{\Delta l}^{\Delta k} + \varphi_{\Delta l}^{\Delta k} = \begin{cases} 2; & \text{if } \Delta k = \Delta l = 0 \\ 0; & \text{otherwise.} \end{cases} \tag{22}$$

Therefore, it is concluded that $\mathbf{\Psi} + \mathbf{\Phi} = 2\boldsymbol{I}_N$. Considering this in (21), one can obtain that $\mathbf{\Lambda}^H\mathbf{\Lambda} = \mathbf{I}_{2N}$, which means that $\mathbf{\Lambda}$ is a unitary matrix.

References

[1] G. Fettweis, M. Krondorf, and S. Bittner, "GFDM—Generalized frequency division multiplexing," in *Proc. IEEE 69th Veh. Technol. Conf. (VTC-Spring)*, Barcelona, Spain, Apr. 2009, pp. 1–4.

[2] N. Michailow *et al.*, "Generalized frequency division multiplexing for 5th generation cellular networks," *IEEE Trans. Commun.*, vol. 62, no. 9, pp. 3045–3061, Sep. 2014.

[3] B. Farhang-Boroujeny and H. Moradi, "OFDM inspired waveforms for 5G," *IEEE Commun. Surveys Tuts.*, vol. 18, no. 4, pp. 2474–2492, 4th Quart., 2016.

[4] M. Matthé, L. L. Mendes, and G. Fettweis, "Generalized frequency division multiplexing in a Gabor transform setting," *IEEE Commun. Lett.*, vol. 18, no. 8, pp. 1379–1382, Aug. 2014.

[5] I. Gaspar, N. Michailow, A. Navarro, E. Ohlmer, S. Krone, and G. Fettweis, "Low complexity GFDM receiver based on sparse frequency domain processing," in *Proc. IEEE 77th Veh. Technol. Conf. (VTC-Fall)*, Dresden, Germany, Jun. 2013, pp. 1–6.

[6] R. Zakaria and D. Le Ruyet, "A novel filter-bank multicarrier scheme to mitigate the intrinsic interference: Application to MIMO systems," *IEEE Trans. Wireless Commun.*, vol. 11, no. 3, pp. 1112–1123, Mar. 2012.

[7] A. Yoshizawa, R. Kimura, and R. Sawai, "A singularity-free GFDM modulation scheme with parametric shaping filter sampling," in *Proc. IEEE 84th Veh. Technol. Conf. (VTC-Fall)*, Montreal, QC, Canada, Sep. 2016, pp. 1–5.

[8] A. Nimr, M. Matthé, D. Zhang, and G. Fettweis, "Optimal radix-2 FFT compatible filters for GFDM," *IEEE Commun. Lett.*, vol. 21, no. 7, pp. 1497–1500, Jul. 2017.

[9] A. Farhang, N. Marchetti, and L. E. Doyle, "Low-complexity modem design for GFDM," *IEEE Trans. Signal Process.*, vol. 64, no. 6, pp. 1507–1518, Mar. 2016.

[10] B. Farhang-Boroujeny, "OFDM versus filter bank multicarrier," *IEEE Signal Process. Mag.*, vol. 28, no. 3, pp. 92–112, May 2011.